Natural Resources for Human Health
eISSN: 2583-1194

Original Research

Received 16 May 2026
Revised 24 June 2026
Accepted 20 July 2026

Natural Resources for Human Health 2026, Vol. 6 (8s): 961–977

KEYWORDS:
Super absorbent hydrogel, chitosan, starch, alginate, acrylamide, methyl acrylate, gum Arabic, polyethylene glycol

Preparation and Characterization of New Super Absorbent Hydrogels Cross-linked Chemically Suitable for Biomedical Applications

Mutaz Zedan Hamed Abed[1,2], Fawzi Habeeb Jabrail[3*]

[1]MSc Research Student in Department of Chemistry, College of Science, University of Mosul, Iraq e-mail: mutaz.24scp138@student.uomosul.edu.iq
[2]Chemical, Biological, and Radiological Safety and Security Section, Presidency of Northern Technical University, Mosul, Iraq. e-mail: moataz.z.hamed@ntu.edu.iq
[3]Polymer research laboratory, Department of Chemistry, College of Science, University of Mosul, Mosul 41002, Iraq. e-mail: fawzijabrail@uomosul.edu.iq
Corresponding author: F. H. Jabrail email: fawzi.jabrail@uomosul.edu.iq

ABSTRACT: The objective of this study is the preparation of new copolymer hydrogels with featured properties such as non-toxic, biocompatible, and biodegradable characteristics that can be used in different biomedical applications. Therefore, the superabsorbent hydrogels were prepared mostly from natural polymers that grafted with synthetic polymers, to improve their mechanical, crystalline, and thermal properties and control the degree of swelling. Six new hydrogels were prepared using chitosan, alginate, and gum Arabic and grafted with starch, poly(ethylene glycol), poly(methyl methacrylate), and polyacrylamide. The hydrogels were characterized using FT-IR, X-ray diffraction, TGA, FESEM, and EDS techniques. All the hydrogels are thermally stable; moreover, the chitosan and alginate hydrogels are semi-crystalline, while gum Arabic hydrogels are amorphous in nature. The FESEM images of the chitosan and alginate hydrogels show rough and undulating surfaces, consisting of homogeneous materials with semi-crystalline sites.

While gum Arabic hydrogels show irregular surfaces containing flakes intertwined with each other, they have dark surfaces without bright areas, providing evidence of amorphous structures.

1. INTRODUCTION

Hydrogels are 3D networks of hydrophilic polymers. They can absorb water and retain massive amounts of water without dissolving [1,2] while remaining solid or semi-solid due to chemical or physical cross-linking. They contain hydrophilic functional groups (like –OH, –NH, and –COOH) that form hydrogen bonds in water, allowing them to swell up and reach thousands of times their dry weight [4]. Hydrogels can hold up to 99% of their weight in water [5], creating a soft, rubbery texture. Hydrogels have distinct properties such as viscoelasticity; they are half solid-like and half liquid-like. In addition, they change volume, shape, or state (sol-gel phase transition) according to external stimuli like temperature, light, pH, electric fields, etc. The hydrogels can spontaneously repair damage occurring to their internal network after physical trauma [6,7]. Most hydrogels are biocompatible, non-toxic, and well-tolerated by living tissues. Hydrogels are classified into natural (like gelatin, collagen, alginate, and chitosan), synthetic like (polyethylene glycol (PEG), and poly(vinyl alcohol) (PVA)), which offer high durability, and hybrid hydrogels that combine natural and synthetic components to balance mechanical strength with bioactivity [8,9].

The cross-linking of hydrogels represents the important process of joining flexible polymer chains together to form a 3D network that traps water. In general, hydrogels are cross-linked physically using weak, non-covalent forces such as hydrogen bonds, ionic charges like sodium hexametaphosphate (SHMP), or hydrophobic loops to link chains. On the other hand, hydrogels are cross-linked chemically with strong, permanent covalent bonds between their chains such as glutaraldehyde and N, N'- methylenebisacrylamide (MBA) [10]. Hydrogels are prepared by turning monomers or water-soluble polymers into a solid or jelly network. The preparation methods use chemical reactions (covalent bonds), physical forces (non-covalent links), or high-energy radiation to lock the hydrophilic molecules together [11]. Referring to two main concepts, the hydrogels are reacted according to their synthesis (cross-linking reactions that form the 3D network) through chemical or physical cross-linking, and according to their environment (stimuli-responsive swelling or shrinking) [12].

There are fundamental differences between physical and chemical hydrogels. Physical hydrogels use reversible, non-covalent bonds making them softer and meltable. Chemical hydrogels often use permanent covalent bonds making them stronger, durable, and stable.

Physical hydrogels have low mechanical strength and tend to break down under heavy stress. They are reversible and can melt or dissolve with changes in pH, heat, or salt levels [13]. The chemical hydrogels have high mechanical strength, stability and durability. Generally, they are irreversible, as they are not melted back into liquid form easily [14]. Finally, hydrogels are highly biocompatible and well suited for drug delivery, embedding living cells, contact lenses, wound dressings, soil water retention and super-absorbent covers in hygiene products [15].

In this study, a number of new hydrogels were prepared and cross-linked chemically.

The prepared hydrogels are chitosan grafted polyethylene glycol (CH-g-PEG), chitosan grafted starch (CH-g-ST), alginate grafted polyethylene glycol (ALG-g-PEG), gum Arabic grafted polyethylene glycol (GA-g-PEG), gum Arabic grafted poly(methyl methacrylate) (GA-g-PMMA), and finally gum Arabic grafted polyacrylamide (GA-g-PAM). N, N'-methylenebisacrylamide (MBA) was used for chemically cross-linking. The prepared hydrogels were characterized using FT-IR, XRD, TGA, FESEM, and EDS techniques.

2. EXPERIMENTAL

2.1 Materials and chemicals

Chitosan (CH) was obtained from Alpha Chemika, Maharashtra, India. Poly(ethylene glycol) (PEG) was purchased from Shilpa Medicare Limited, Ambatapur, India. The compounds N, N'-methylenebisacrylamide (MBA), acetic acid, sodium alginate (ALG), gum Arabic (GA), methyl methacrylate (MMA), ammonium persulphate (APS), benzaldehyde, sodium hydroxide, hydrochloric acid, n-heptane, sodium bicarbonate, ferric chloride, and calcium chloride were obtained from BDH Brighouse, UK. Acrylamide (AM), starch (ST), and pyrogallol were purchased from Fluka, Geneva, Switzerland. Ascorbic acid, ceric ammonium nitrate, and dimethyl sulfoxide (DMSO) were supplied by Sigma-Aldrich.

2.2 Preparation of hydrogels

2.2.1 Preparation of (CH-g-PEG)/MBA copolymer hydrogel

A 2 g sample of chitosan was dissolved in 200 mL of (2 v/v) acetic acid solution. The mixture was stirred gently for 3 hours at room temperature and its pH was kept between 3.6 and 5.6. A 2 g sample of PEG was dissolved in 100 mL DMSO, and the solution was transferred into a 500 mL round bottom flask. A 2.4 mL sample of benzaldehyde was added with a few drops of concentrated HCl. The final mixture was heated for 8 hours to 80°C with stirring and was finally neutralized with NaOH solution. The organic layer was washed several times with water or a saturated sodium bicarbonate solution for impurity removal, and then the product was dried at room temperature. The produced acetal-PEG product was dissolved in 150 mL of acetic buffer solution with a pH of 3.6 to 5.6. The acetal-PEG solution was added to the chitosan solution in a 500 mL three-neck round flask. The reflux system was connected to a nitrogen line passed through alkaline pyrogallol solution to remove oxygen. The reacted materials were heated to 60°C with stirring for 6 hours. A sample of ascorbic acid (2 g) as a reducing agent was added to the reaction mixture. The reacted materials were heated to 90°C for 2 hours with stirring to complete the grafting process. For cross-linking, a 2 g sample of N, N'-methylenebisacrylamide (MBA) was added and the heat was reduced to 60°C

for 1 hour with stirring. Then, the heat was stopped, but stirring was continued for another hour. The precipitate was collected, washed with distilled water several times, and then dried at room temperature.

2.2.2 Preparation of (CH-g-ST)/MBA copolymer hydrogel

A sample of chitosan (2 g) was dissolved in 200 mL of a 2% v/v acetic acid solution. The mixture was kept at pH 3.6–5.6 with stirring for 3 hours at room temperature. A solution of starch (ST) in distilled water D.W. was prepared by dissolving 2 g of ST in 20 mL of D.W. and heated to 50°C for 30 minutes with stirring. In a 250 mL three-neck round flask, the two mixtures were combined, and 20 mL of a 5% w/v aqueous solution of ceric ammonium nitrate (CAN) was added to initiate the grafting reaction. The reflux system was connected to a nitrogen gas line passed through an alkaline pyrogallol solution, and its contained compounds were heated to 90°C for 2 hours with stirring for the grafting reaction. A 2 g sample of MBA for chemical cross-linking was added, and the solution was heated to 60°C for hour with stirring. Then the heat was stopped, and stirring was continued for additional hour. The formed precipitate was washed several times with D.W. and then dried at room temperature.

2.2.3 Preparation of (ALG-g-PEG) copolymer hydrogel

A 2 g sample of sodium alginate (ALG) was dissolved in 100 mL of D.W., and a viscous solution was formed. A 2 g sample of PEG in 100 mL of D.W. was prepared. The alginate and PEG mixtures were transferred into a 500 mL three-neck round flask, which was connected to a nitrogen gas line that passed through alkaline pyrogallol solution. A 1.23 g sample of ammonium persulfate (APS) was added as an initiator. The reflux mixture was heated to 70°C for 2 hours with stirring to facilitate the formation of free radicles in the alginate backbone, which enabled the grafting of PEG onto the alginate chains. The mixture components were kept under stirring for an extended period of 3 hours at a controlled temperature of 50°C. A 2 g sample of MBA cross-linker was added with stirring and the temperature was maintained at 45°C for 150 minutes. The formed precipitate was collected, washed, and dried at room temperature.

2.2.4 Preparation of (GA-g-PEG)/MBA copolymer hydrogel

A 2 g sample of gum Arabic was prepared as a clear solution in 100 mL of D.W. On the other hand, the PEG solution was prepared using 2 g of PEG in 100 mL of D.W. The two solutions were mixed inside a 500 mL three-neck round flask, which was already connected to a nitrogen gas line passed through alkaline pyrogallol solution. The initiator APS was added as 20 mL sample of 5% w/v, and the final solution was heated to 70°C for 2 hours with stirring. A 1 g sample of MBA cross-linker was added, and the mixture was kept at 70°C for another 2 hours with stirring. Then the heat was stopped while continuing stirring for another hour. The precipitate product was collected, washed several times with D.W., and dried at room temperature.

2.2.5 Preparation of (GA-g-PMMA)/MBA copolymer hydrogel

A 3.8 mL sample of methyl methacrylate (MMA) monomer was transferred into a 250 mL three-neck round flask. A 2 g sample of gum Arabic was dissolved in 100 mL of D.W. and added to the MMA monomer. The flask was connected to a nitrogen gas line passed through alkaline pyrogallol solution. A 20 mL sample of APS initiator prepared in a 5% w/v aqueous solution was added to the flask and the final mixture was heated to 70°C for 1 hour with stirring. A 2 g sample of MBA cross-linker was added, and the temperature of the mixture was kept at 70°C for another hour with stirring. Then heating was stopped, and stirring was continued for an extra hour. The formed precipitate was collected, washed several times with D.W., and dried at room temperature.

2.2.6 Preparation of (GA-g-PAM)/MBA copolymer hydrogel

A 2 g sample of GA was prepared in 100 mL of D.W. and added together with a solution of acrylamide (AM) monomer prepared by dissolving 2 g in 100 mL of D.W. A 250 mL three-neck round flask was used for the reflux reaction connected, to a nitrogen gas line passed through alkaline pyrogallol solution. 20 mL of 5% w/v APS initiator was added, and the flask was heated to 70°C for hour with stirring. A 1 g sample of MBA cross-linker was added, and the temperature was continued at 70°C for hour with stirring. Then heat was stopped but stirring was kept for an extra hour. The formed precipitate product was collected, washed several times with D.W, and dried at room.

3. RESULTS AND DISCUSSION

Hydrogels are prepared because of their unique, water-swollen polymer networks, offering incredible versatility for medical treatments, mimicking living soft tissues, sustainable agriculture and releasing medicine slowly or under the effects of some stimuli, such as heat, pH, and light. Hydrogels are synthesized in order to create flexible 3D networks of hydrophilic polymer chains that have the ability to absorb and retain massive amounts of water.

Six different types of copolymer hydrogels were prepared from natural and synthetic polymers and synthetic monomers. The prepared polymers were characterized using a number of techniques, including FT-IR, XRD, TGA, FESEM, and EDS.

3.1 Characterization of the prepared hydrogels

3.1.1 FT-IR spectroscopy

The FT-IR spectrum of the (CH-g-PEG)-MBA copolymer hydrogel, the name of which has been abbreviated in the following form CPE-MBA (Figure 3.1 and Table 3.1), shows that the absorption frequency 3339 cm^{-1} belongs to (-OH) groups in chitosan. The peak at 1628 cm^{-1} represents amide I groups of chitosan [16] and the carbonyl groups of MBA.

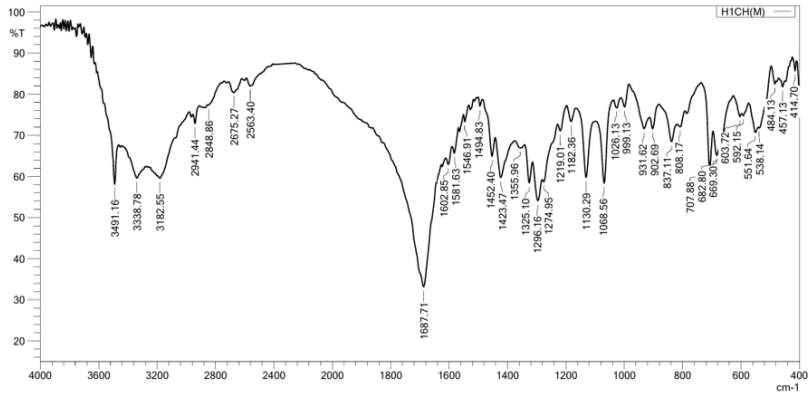

Figure 3.1: FT-IR spectrum of CPE-MBA copolymer hydrogel.

The peak at 1547 cm^{-1} belongs to amide II of chitosan [17].

Table 3.1: FT-IR absorption frequencies of the hydrogel's functional groups

Hydrogel	FT-IR Characteristic Functional Groups							
	ν(O-H)str	ν(C-H)str	ν(C=O)str	ν(N-H)def	ν(C=O)str Asym/Sym	ν(C-O)str	ν(C-N)bend	δ(C-O-H)def
CPE-MBA	3339	2947, 2849	1698	1547	1423	1026	1130	1325
CST-MBA	3334	2936, 2872	1634	1556	1404	1023	1145	1324
APE-MBA	3197	3043, 2867	1644	1528	1410	1024	1125	1298
GPE-MBA	3226	2926, 2880	1643	1526	1403	1045	1179	1296
GPM-MBA	3289	2948, 2850	1729, 1644	1525	1446	1045	1147	1380
GPA-MBA	3204	3063, 2926	1644	1523	1442	1043	1183	1392

The FT-IR spectrum of the (CH-g-ST)/MBA hydrogel, the name of which has been abbreviated in the following form CST-MBA (Figure 3.2 and Table 3.1), shows that the peak at 3334 cm^{-1} belongs to (-OH) groups of both chitosan and starch polymers. The peak at 1634 cm^{-1} represents the amide I of chitosan as well as the carbonyl groups of MBA. The band at 1556 cm^{-1} represents the amide II of chitosan [18].

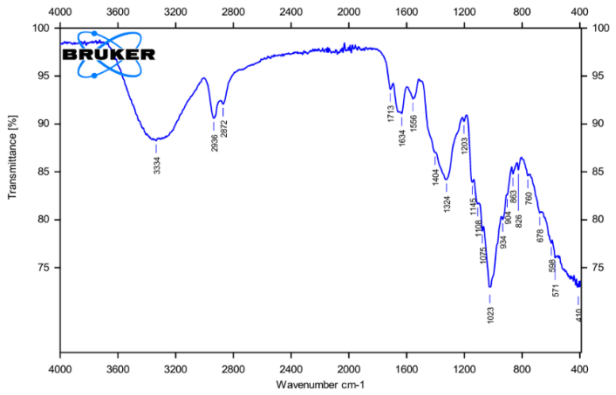

Figure 3.2: FT-IR spectrum of CST-MBA copolymer hydrogel.

The FT-IR spectrum of (ALG-PEG)/MBA hydrogel, abbreviated as APE-MBA copolymer hydrogel (Figure 3.3 and Table 3.1), shows that the peak at 3197 cm^{-1} represents the hydroxy groups of alginate. The peak at 1644 cm^{-1} belongs to the carbonyl groups (C=O) of alginate and MBA [19]. The absorption frequency at 1528 cm^{-1} represents the (N-H)def group of MBA.

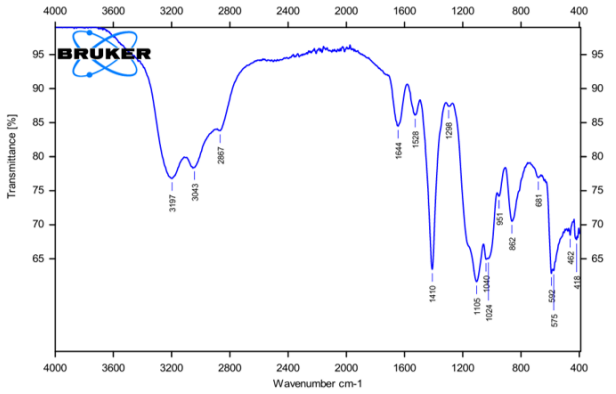

Figure 3.3: FT-IR spectrum of APE-MBA copolymer hydrogel.

The FT-IR spectrum of (GA-g-PEG)/MBA hydrogel, abbreviated as GPE-MBA hydrogel (Figure 3.4 and Table 3.1), shows that the peak at 3226 cm^{-1} belongs to the hydroxyl group (-OH) of gum Arabic. The peak at 1643 cm^{-1} represents the carbonyl groups (C=O) of gum Arabic and MBA [20]. The peak at 1526 cm^{-1} belongs to (N-H) groups of MBA.

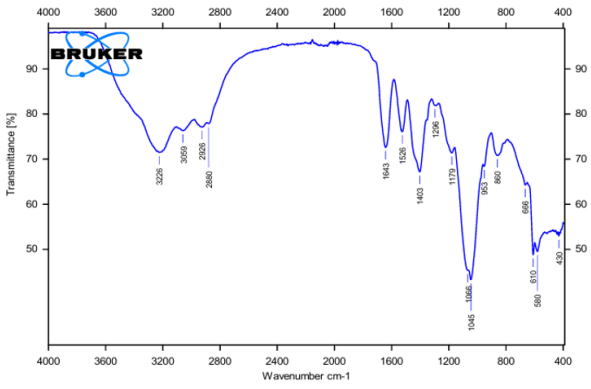

Figure 3.4: FT-IR spectrum of GPE-MBA copolymer hydrogel.

The FT-IR spectrum of (GA-g-PMMA)/MBA copolymer hydrogel, abbreviated as GPM-MBA (Figure 3.5 and Table 3.1), shows that the absorption frequency at 3289 cm^{-1} belongs to the (-OH) groups of gum Arabic. The peak at 1729 cm^{-1} belongs to the carbonyl groups (C=O) of PMMA which is heavily influenced by the adjacent methoxy group [21]. The absorption frequencies at 1644 cm^{-1} and 1525 cm^{-1} belong to the carbonyl groups (C=O) and amide II (-NH) groups of MBA. The peak at 1147 cm^{-1} belongs to (C-N) and (C-O-C) units, representing an asymmetric band for the ester functional group linking to the methoxy oxygen [22].

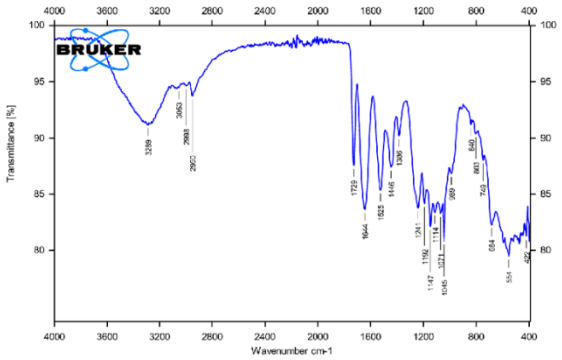

Figure 3.5: FT-IR spectrum of GPM-MBA copolymer hydrogel.

The FT-IR spectrum of the (GA-g-PAM)/MBA copolymer hydrogel, abbreviated as GPA-MBA (Figure 3.6 and Table 3.1), shows that the peak at 3204 cm^{-1} belongs to the (-OH) groups of gum Arabic. The absorption frequency at 1644 cm^{-1} represents the carbonyl groups (C=O) of gum Arabic, the amide I band of PAM, and those of MBA. The peak at 1523 cm^{-1} belongs to the amide II of PAM and MBA.

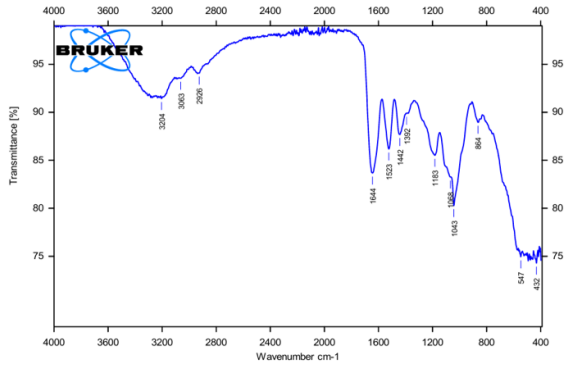

Figure 3.6: FT-IR Spectrum of GPA-MBA copolymer hydrogel.

3.1.2 X-ray diffraction

The X-ray diffraction (XRD) is used to determine the degree of crystallinity and crystal structure of the studied materials. The XRD pattern of the CPE-MBA hydrogel (Figure 3.7) shows that chitosan is a semi-crystalline compound that was grafted with PEG, which also has a semi-crystalline structure, and cross-linked with crystalline MBA. As a result, the formed hydrogel shows a semi-crystalline structure (Figure 3.7) containing 27 crystalline peaks. However, chitosan shows main peaks that appear between 11.16° and 20.63° along the 2θ axis, while PEG gives peaks at 19.04° and 23.34° along the 2θ axis. The main peak of MBA is at 25.80° along the 2θ axis [23-25].

Natural Resources for Human Health
eISSN: 2583-1194

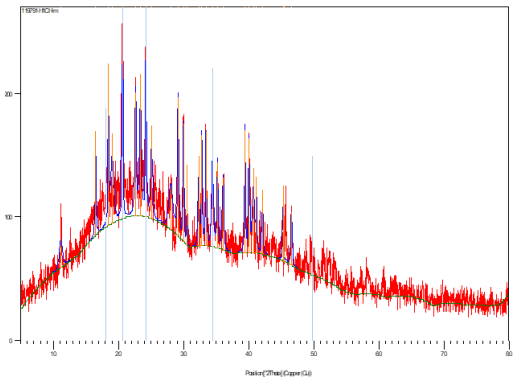

Figure 3.7: XRD pattern of CPE-MBA copolymer hydrogel.

The XRD pattern of the CST-MBA copolymer hydrogel (Figure 3.8) shows two main broad peaks close to each other, located between 25.35° and 45.51° along the 2θ axis, indicate that the hydrogel has a semi-crystalline configuration, as they overlap with each other.

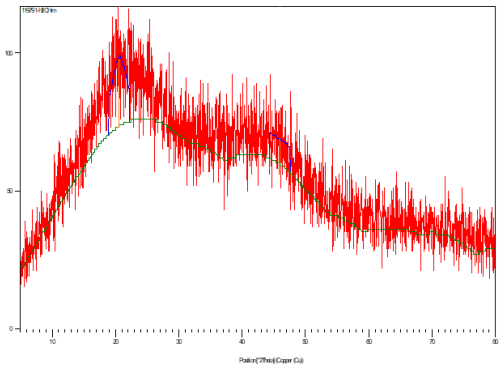

Figure 3.8: XRD pattern of CST-MBA copolymer hydrogel.

The XRD pattern of the APE-MBA copolymer hydrogel (Figure 3.9) shows that alginate has a characteristic main primary peak at 23.58° along the 2θ axis, and broad diffraction halos represent a secondary peak that mainly appears at 17.82° along the 2θ axis [26]. The peak of PEG was observed at 19.07° along the 2θ axis, while the peak that appeared at 26.20° along the 2θ axis is from MBA. Finally, the XRD pattern (Figure 3.9) shows that the hydrogel has a partially crystalline configuration.

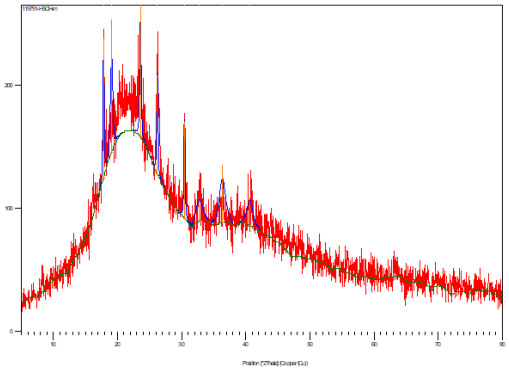

Figure 3.9: XRD pattern of APE-MBA copolymer hydrogel.

The XRD pattern of the GPE-MBA copolymer hydrogel (Figure 3.10) shows that the hydrogel has an amorphous nature. The sample shows a broad peak appearing at 19.09° along the 2θ axis, which belongs to PEG and another small peak at 24.8° along the 2θ axis that is from the MBA compound.

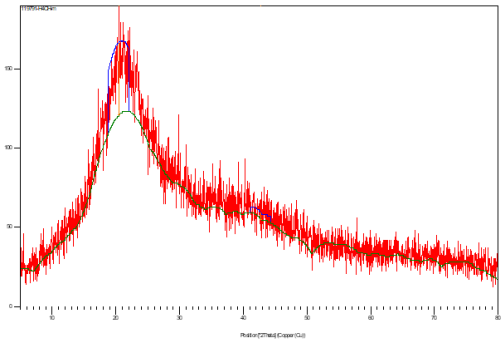

Figure 3.10: XRD pattern of GPE-MBA copolymer hydrogel.

The XRD pattern of the GPM-MBA copolymer hydrogel (Figure 3.11) shows that the nature of the hydrogel is amorphous. However, gum Arabic shows a broad diffuse halo peak centered between 12.0° and 25.0° along the 2θ axis. Therefore, three broad peaks appeared for the GPM-MBA hydrogel (Figure 3.11) as follows: 12.79°, 21.88°, and 42.05° along the 2θ axis, representing gum Arabic, MBA, and PMMA, respectively [27].

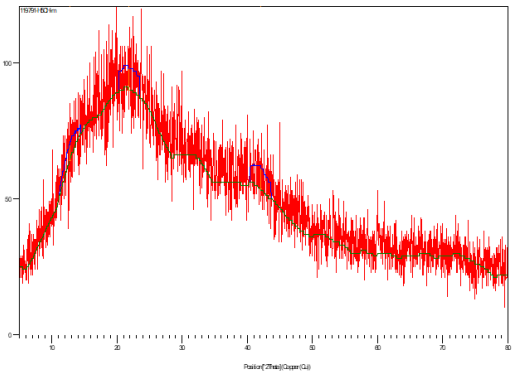

Figure 3.11: XRD pattern of GPM-MBA copolymer hydrogel.

The XRD pattern of the GPA-MBA copolymer hydrogel (Figure 3.12) shows that the hydrogel has an amorphous nature with a broad diffuse halo centered at 20.28° along the 2θ axis belonging to PAM [28]. Accordingly, the hydrogel has shown an amorphous structure.

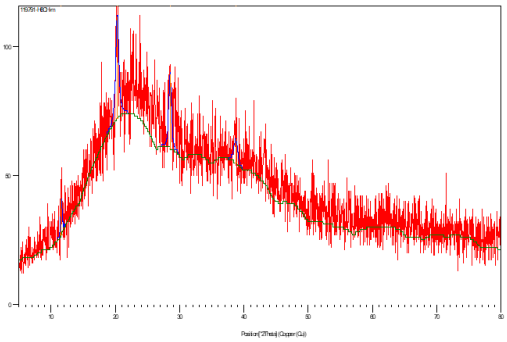

Figure 3.12: XRD pattern of GPA-MBA copolymer hydrogel.

Natural Resources for Human Health
eISSN: 2583-1194

3.1.3 TGA thermal analysis

The TGA thermogram of the CPE-MBA copolymer hydrogel (Figure 3.13 and Table 3.2) shows a weight loss of 0.5% at an initial decomposition temperature (IDT) of 283.0°C, which means the hydrogel is thermally stable [29]. Moreover, the hydrogel records a weight loss of 2.0% at the maximum decomposition temperature (Tmax) of 429.0°C, which indicates that the hydrogel is thermally stable, and at its crystalline decomposition temperature (CT) of 520.0°C, the hydrogel losses only 38.5% of its total weight. In addition, the hydrogel shows a final decomposition temperature (FDT) of 591.0°C with a weight loss of only 43.0% only [30].

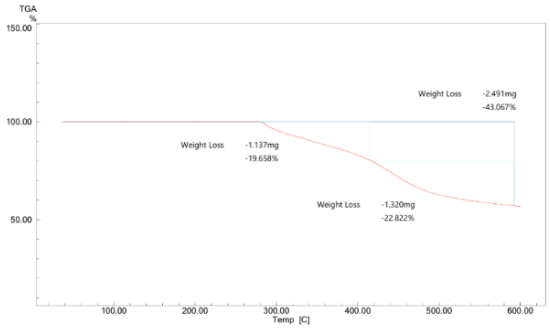

Figure 3.13: TGA thermogram of CPE-MBA copolymer hydrogel.

The TGA thermogram of the CST-MBA copolymer hydrogel (Figure 3.14 and Table 3.2) shows that the hydrogel exhibits a weight loss of 1.56% at an IDT of 43.0°C and a weight loss of 30.0% at Tmax of 282.0°C, which indicating that the hydrogel is thermally stable [31]. Moreover, the hydrogel shows a weight loss of 56.5% at Tcr of 480.0°C, which suggests that the hydrogel is stable; particularly it exhibits a weight loss of 60.0% at a high FDT of 597.0°C [32].

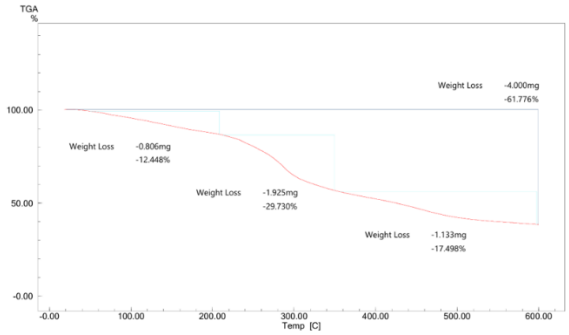

Figure 3.14: TGA thermogram of CST-MBA copolymer hydrogel.

Table 3.2: TGA thermal analysis data of the prepared polymer hydrogels.

Hyrogel	Wight loss (%)	IDT (°C)	Weight loss (%)	Tmax (°C)	Weight loss (%)	Tcr (°C)	Weight loss (%)	FDT (°C)
CPE-MBA	0.5	283.0	21.0	422.0	38.5	520.0	43.0	591.0
CST-MBA	1.56	43.5	30.0	282.0	56.5	480.0	60.0	597.0
APE-MBA	1.25	37.5	32.5	280.0	57.5	409.5	64.5	587.5
GPE-MBA	1.35	39.0	30.0	303.5	57.5	422.0	62.0	592.0
GPM-MBA	0.80	46.0	37.0	347.5	66.5	453.0	73.5	588.0
GPA-MBA	0.60	48.0	32.0	273.5	42.5	443.0	63.5	790.0

The TGA thermogram of the APE-MBA copolymer hydrogel (Figure 3.15 and Table 3.2) shows that the hydrogel has a weight loss of 1.25% at an IDT of 37.5°C and a weight loss of 32.5% at a Tmax of 280.0°C. Moreover, the hydrogel shows a weight loss of 57.5% at a Tcr of 409.5°, which means the hydrogel is thermally stable, and this is why it losses only 64.5% at an FDT of 587.5°C [33].

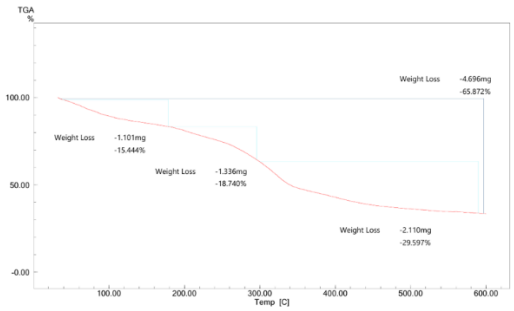

Figure 3.15: TGA thermogram of APE-MBA copolymer hydrogel.

The TGA thermogram of the GPE-MBA copolymer hydrogel (Figure 3.16 and Table 3.2) shows that the hydrogel has a weight loss of 1.35% at IDT of 39.0°C and a weight loss of 30.0% at Tmax of 303.5°C. In general, the hydrogel shows a thermally stable structure according to its weight losses of 57.5% and 62.0% at Tcr of 422.0°C and FDT of 592.0°C, respectively [34, 35].

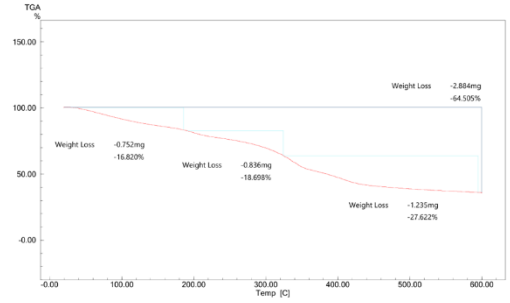

Figure 3.16: TGA thermogram of GPE-MBA copolymer hydrogel.

The TGA thermogram of the GPM-MBA copolymer hydrogel (Figure 3.17 and Table 3.2) shows that the hydrogel has a weight loss of 0.80% at IDT of 46.0°C and a weight loss of 37.0% at Tmax of 343.5°C. In addition, the weight loss of 66.5% at Tcr of 453.0°C gives a weight loss of 73.5% at FDT of 588.0°C, which means the hydrogel is thermally stable [34, 36].

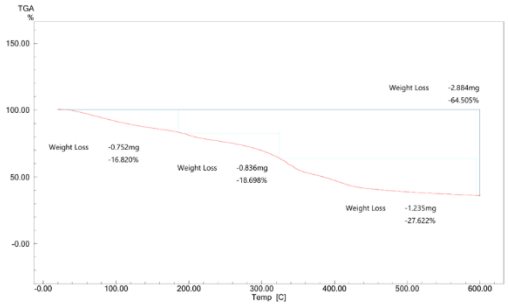

Figure 3.17: TGA thermogram of GPM-MBA copolymer hydrogel.

The TGA thermogram of the GPA-MBA copolymer hydrogel (Figure 3.18 and Table 3.2) shows that the hydrogel has a weight loss of 0.60% at an IDT of 48.0°C and a weight loss of 32.0% at Tmax of 273.5°C. Moreover, the hydrogel shows a weight loss of 42.5% at Tcr of 443.0°C and a weight loss of 49.5% at FDT of 443.0°C, which means the hydrogel has good thermal stability [37-38].

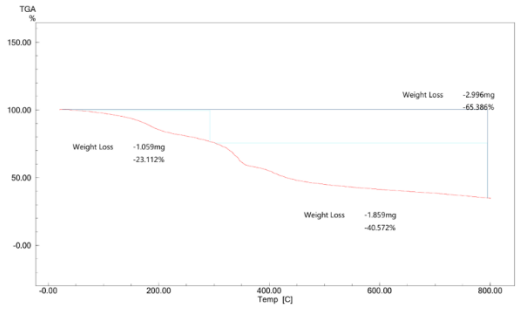

Figure 3.18: TGA thermogram of GPA-MBA copolymer hydrogel.

3.1.4 FESEM and EDS analysis

The FESEM image of the CPE-MBA copolymer hydrogel (Figure 3.19) shows a non-smooth surface of homogeneous hydrogel. The hydrogel components appeared cohesive and contiguous with bright white areas representing the semi-crystalline structure of the hydrogel [39].

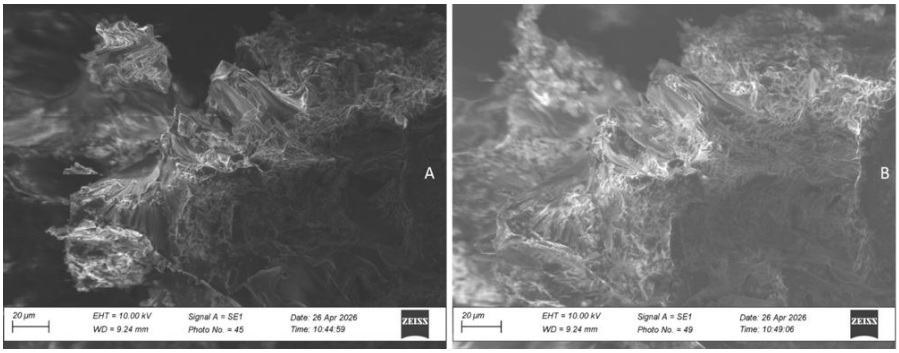

Figure 3.19: FESEM images of CPE-MBA copolymer hydrogel (a)and(b)images represent different regions of the sample.

The EDS image of the CPE-MBA hydrogel (Figure 3.20) shows that the hydrogel mainly contains carbon, oxygen, and nitrogen, with traces of sodium present from the deacetylation of chitin.

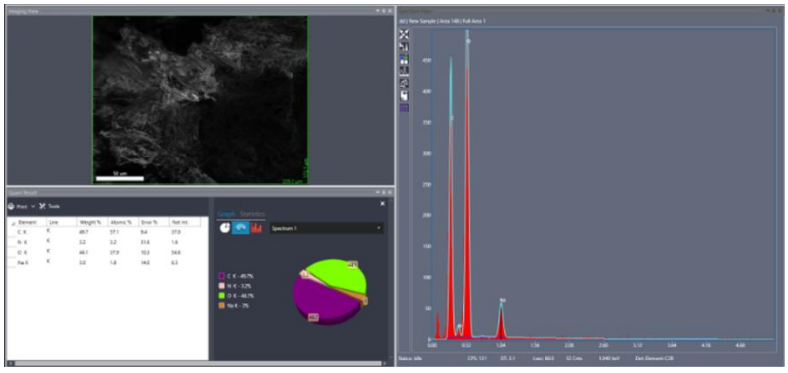

Figure 3.20: EDS image of CPE-MBA copolymer hydrogel.

The FESEM image of the CST-MBA copolymer hydrogel (Figure 3.21) shows a rough and undulant hydrogel surface with many holes and folds. The bright white areas belong to the semi-crystalline structure of the hydrogel [40].

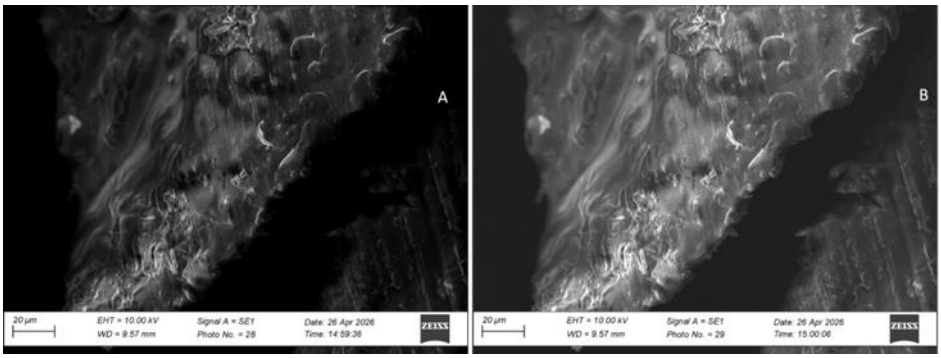

Figure 3.21: FESEM images of CST-MBA copolymer hydrogel (a) and (b) images represent different regions of the sample.

The EDS image of the CST-MBA copolymer hydrogel (Figure 3.22) shows that the hydrogel consists of pure materials, containing carbon, oxygen, and nitrogen with no other elements.

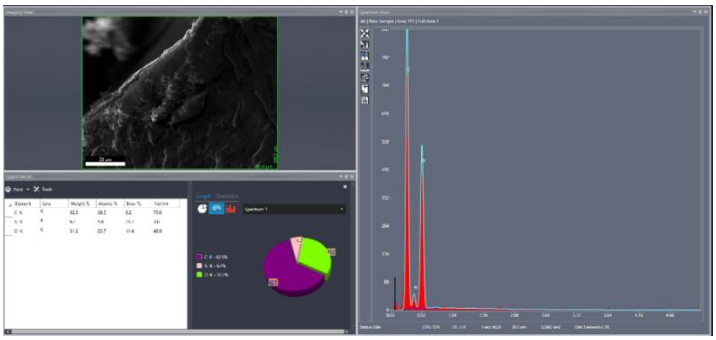

Figure 3.22: EDS image of CST-MBA copolymer hydrogel.

The FESEM image of the APE-MBA copolymer hydrogel (Figure 3.23) shows that the hydrogel surface is clearly rough, jagged, and contains many holes and folds. In addition, the hydrogel surface is filled with protrusions that contain many pores. The bright white areas covering most of the hydrogel surface indicate that the hydrogel has a semi-crystalline composite [41-42].

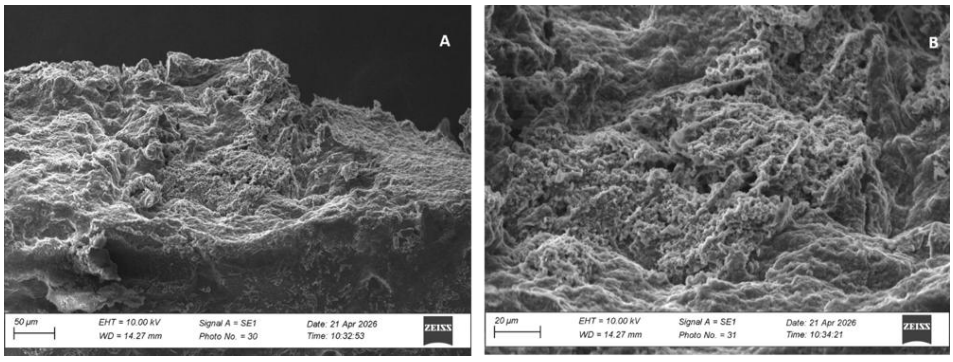

Figure 3.23: FESEM images of APE-MBA copolymer hydrogel (a) and (b) images represent different regions of the sample.

The EDS image of the APE-MBA copolymer hydrogel (Figure 3.24) shows that the hydrogel contains carbon, oxygen, nitrogen, and sulfur. The first three elements are part of the hydrogel composite, while the sulfur element is often introduced through the sulfur-containing persulfate initiator used to trigger the reaction [43].

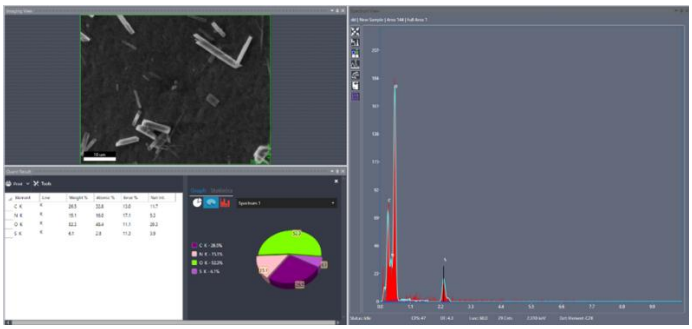

Figure 3.24: EDS image of APE-MBA copolymer hydrogel.

The FESEM image of the GPE-MBA copolymer hydrogel (Figure 3.25) shows that the hydrogel has a discontinuous and irregular surface that contains flakes intertwined with each other. The bright white areas have disappeared in the FESEM image of the GPE-MBA hydrogel, which means the hydrogel has an amorphous nature [44].

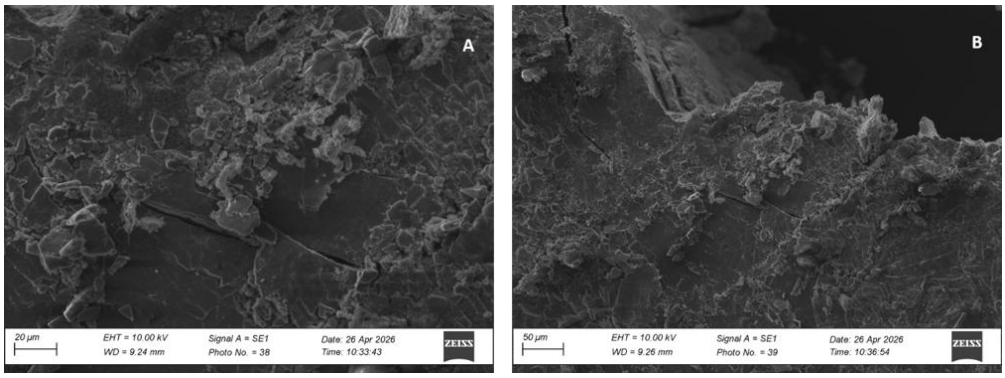

Figure 3.25: FESEM images of GPE-MPA copolymer hydrogel (a) and (b) images represent different regions of the sample.

The EDS image of the GPE-MBA copolymer hydrogel (Figure 3.26) shows that the hydrogel contains carbon, oxygen, nitrogen, sulfur, and potassium elements. The sulfur element remained from the initiator, while the potassium element is typically present in the hydrogel; it stems from the natural composition of gum Arabic itself [45].

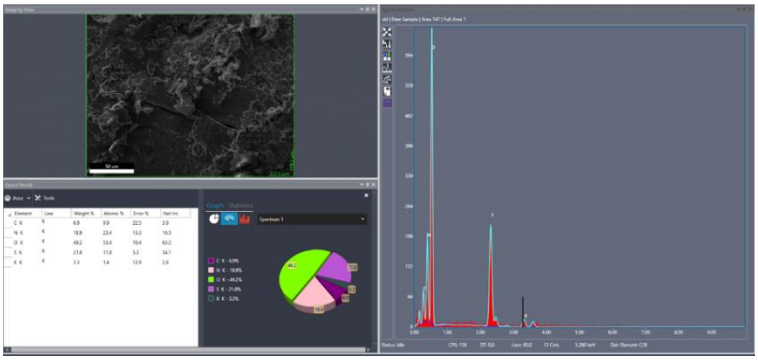

Figure 3.26: EDS image of GPE-MBA copolymer hydrogel.

The FESEM image of the GPM-MBA copolymer hydrogel (Figure 3.27) shows that the hydrogel has a cross-sectioned surface with interconnected flakes scattered on its surface. The hydrogel is filled with folds and cracks spread across its surface. The irregular interlined flakes prove the hydrogel was grafted and cross-linked [46]. Moreover, the hydrogel shows no bright white areas, meaning the hydrogel is amorphous.

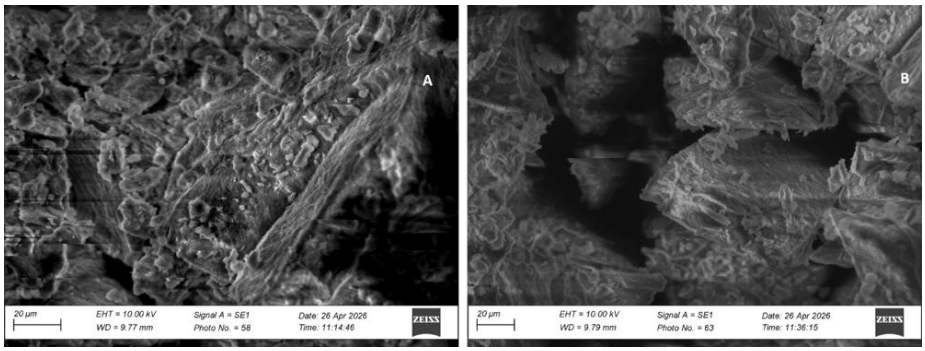

Figure 3.27: FESEM images of GPM-MBA copolymer hydrogel (a) and (b) images represent different regions of the sample.

The EDS image of the GPM-MBA copolymer hydrogel (Figure 3.28) shows the hydrogel contains carbon, oxygen, and nitrogen, which are the main elements of the hydrogel and traces of sulfur, which come from the initiator.

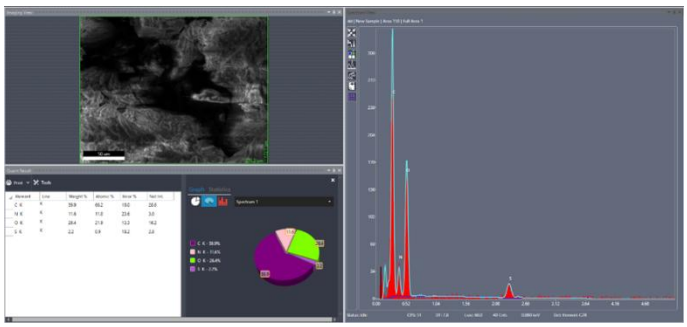

Figure 3.28: EDS image of GPM-MBA copolymer hydrogel.

Finally, the FESEM image of the GPA-MBA copolymer hydrogel (Figure 3.29) shows a homogeneous surface of the hydrogel that contains overlapping folds and zigzags, as well as pores distributed on the hydrogel surface. The FESEM image shows no bright white areas on the hydrogel surface, which means the hydrogel is amorphous [47].

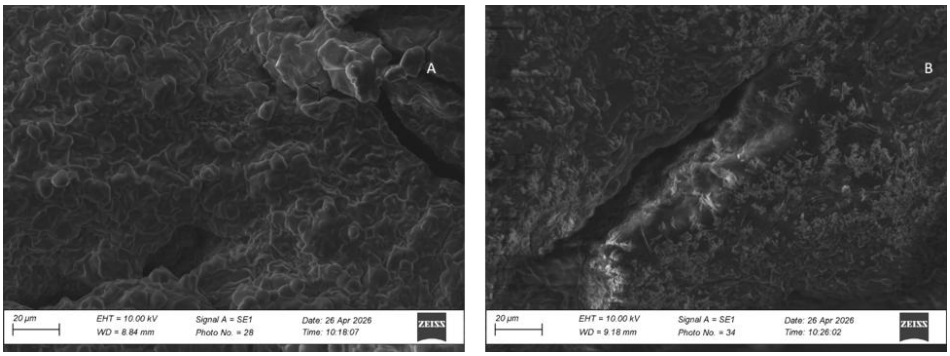

Figure 3.29: FESEM images of GPA-MBA copolymer hydrogel (a) and (b) images represent different regions of the sample.

The EDS image of the GPA-MBA copolymer hydrogel (Figure 3.30) shows that the hydrogel contains carbon, oxygen, nitrogen, sulfur, and potassium elements. The last two elements come from the initiator and gum Arabic, respectively.

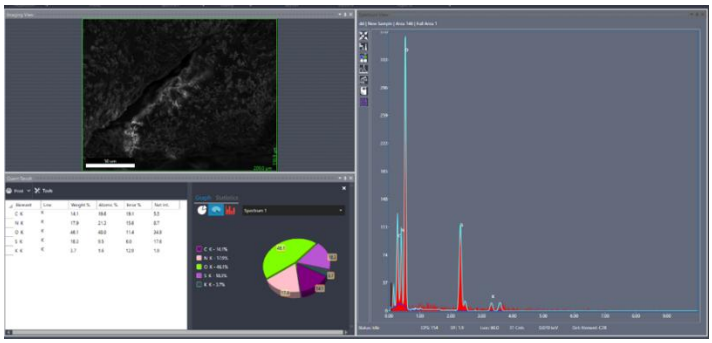

Figure3.30: EDS image of GPA-MBA copolymer hydrogel.

3.2 Uses and applications of the prepared hydrogels

The main properties of the hydrogel are three-dimensional networks of hydrophilic polymers, soft materials, and the ability to absorb and retain large amounts of water, reaching thousands of times their dry weight while remaining insoluble due to chemical or physical cross-linking. Because of these distinct properties, hydrogels will have many applications in virous fields, including industrial, medical, agricultural, water desalination, and others. Prepared hydrogels which are CPE-MBA, CST-MBA, APE-MBA, GPE-MBA, GPM-MBA, and GPA-MBA were examined and their chemical compositions, crystalline structures, thermal stability and surface morphology were investigated. The CPE-MBA, CST-MBA, and APE-MBA hydrogels show semi-crystalline configurations, are thermally stable, and have rough and undulanting surface morphologies containing a large number of holes and folds. Therefore, these hydrogels are suitable for advanced technologies like self-healing materials, shape-memory devices, smart 3D printing inks, and injectable medical gels.

On the other hand, the GPE-MBA, GPM-MBA, and GPA-MBA hydrogels have shown a discontinuous and irregular surface that contains interconnected flakes scattered on it. Moreover, the hydrogels are thermally stable and have an amorphous structure. Therefore, these hydrogels are highly useful for targeted drug delivery, tissue regeneration scaffolds, and efficient wound hydration.

4. CONCLUSIONS

New hydrogels were prepared using different polymers. The preparation process includes grafting of natural polymers like chitosan, alginate, and gum Arabic with natural polymers like starch, or synthetic polymers like poly(ethylene glycol), poly(methyl methacrylate), and polyacrylamide. All prepared hydrogels were cross-linked with N, N'-methylenebisacrylamide. Modern and sophisticated chemical procedures have been used to prepare new copolymer hydrogels.

The hydrogels were characterized using FT-IR spectroscopy; all their structures have been verified based on their functional groups. The X-ray diffraction analysis shows the CPE-MBA, CST-MBA, and APE-MBA hydrogels have semi-crystalline configurations, while GPE-MBA, GPM-MBA, and GPA-MBA hydrogels have amorphous structures.

The prepared hydrogels show thermal stability at high temperatures, and their weight loss percentages at Tmax and Tcr were acceptable at high decomposition temperatures. The scanning electron microscope images of the hydrogels, surfaces are filled with holes and folds, and the bright white areas are shown only in the FESEM images of CPE-MBA, CST-MBA, and APE-MBA hydrogels.

The EDS analysis shows the prepared hydrogels mainly consist of carbon, oxygen, and nitrogen elements. Some samples show the presence of sulfur, which comes from the remainder of the initiator, or potassium, which is a natural component of gum Arabic.

Acknowledgements: The authors acknowledge chemistry department, college of science, University of Mosul for supporting the work.

Author Contributions: The author Fawzi HJ supervised the work, contributed to the methodology, The author Mutaz ZHA was responsible for hydrogels preparation, data collection and investigations. Both authors have read and approved the final manuscript.

Conflict of Interest: The authors declare no conflict interests.

REFERENCES

[1] Rana T, Fatima M, Khan AQ, et al. Hydrogel: A novel drug delivery system. J Biomed Res Environ Sci. 2020;1(8):439–451.
[2] Tiwari SV, Dabhade SV. A study of hydrogels. Acta Sci Pharm Sci. 2021; 5(6):86–94.
[3] Metha P, Sharma M, Devi M. Hydrogels: An overview of its classifications, properties, and applications. J Mech Beh Biomed Mat. 2023; 147: 106445.
[4] Priya AS, Premanand R, Ragupathi I, et al. Comprehensive review of hydrogel synthesis, characterization and emerging applications. J Compos Sci. 2024; 8(11):457.
[5] Kulkarni N, Rao P, Jadhav GS, Kulkarni B, et al. Emerging role of injectable dipeptide hydrogels in biomedical applications. ACS Omega. 2023; 8(4):3551–3570.
[6] Khan MUA, Aslam MA, Abdulla MEB, et al. Hydrogels: Classifications, fundamental properties, applications, and scopes in recent advances in tissue engineering and regenerative medicine—A comprehensive. Arab J Chem. 2024;17(10):105968.
[7] Bashir S, Hina M, Iqbal J, Rajpar AH, et al. Fundamental concepts of hydrogels: Synthesis, properties, and their applications. Polymers. 2020;12(11):2702.
[8] Shariati FS, Ebrahimi T, Shariati A, Maghsood M, et al. Hydrogels: Properties, classifications, characterization and biomedical applications. Clinical Res Stud. 2025; 4(5):1–10.
[9] Ho TC, Chang CC, Chan HP, Chung TW, et al. Hydrogels: Properties and applications in biomedicine. Molecules. 2022; 27(9):2902.
[10] Kumar A, Pandey S, Tungala K. Hydrogels: classification, cross-linking methods, characteristics, and current trends in biomedical applications. Polym. Bull. 2026; 83(14).
[11] Priya AS, Premanand R, Ragupathi I, et al. Comprehensive review of hydrogel synthesis, characterization and emerging applications. J. Compos. Sci. 2024; 8(11):457.
[12] Pan S, Zhu C, Tao L. Hydrogels constructed by multicomponent reactions. Polym. Chem. 2024;15(47):4799–4809.
[13] Siqueira EC, Franca JAA, Souza RFM, et al. Recent advances in the development of the physically crosslinked hydrogels and their biomedical applications. Res. Soc. Dev. 2023;12(8): e18212843073.
[14] Rebers L, Reichsollner R, Southan A. Differentiation of physical and chemical cross-linking in gelatin methacryloyl hydrogels. Sci. Rep. 2021; 11:3256.
[15] Rybicki M, Czajkowska K, Grochowska A, et al. Innovative applications of hydrogels in contemporary medicine. Gels. 2025;11(10):798.
[16] Al-Bana LR, Al-Khatib AR, Jabrail FH. Antibacterial and remineralizing effects of orthodontic adhesive modified by nano-chitosan loaded with calcium phosphate. Braz. Dent. Sci. 2024;24(4): e4552.
[17] Rehman HV, Cord-Landwehr S, Shapaval V, et al. High-throughput vibrational spectroscopy methods for determination of degree of acetylation for chitin and chitosan. Carbohydr. Polym. 2023; 302:120428.
[18] Al-Bana LR, Al-Khatib AR, Jabrail FH. Evaluation of the biological, physical, mechanical and chemical properties of orthodontic primer modified by nano-chitosan loaded with bioactive materials. J. Oral Biol. Craniof. Res. 2025; 15:500-507.
[19] Donat I, Christensen BE. Alginate-metal cation interactions: Macromolecular approach. Carb. Polym. 2023; 321:121280.
[20] Adam AA, Jasniewski J, Vuillemin ME, et al. Enzymatic mediated modification of gum Arabic by curcumin oxidation product: Physicochemical and self-assembly study. Food Hydrocol. 2022; 126:107451.
[21] Smith BC. Infrared spectroscopy of polymers X: Polyacrylates. Spectro. 2023;38(1):10–14.
[22] Megaled ON, Abdelhamid MI, El Wassefy NA, Youssef AM, et al. Fabrication and characterization of polymethyl methacrylate (PMMA) matrix modified with strontium nano-rods. Sci. Rep. 2026; 16:9342.
[23] George T, Ghosh R, Joseph LM, Chowdhury S, et al. Crystallization of low-dimensional lead-free $(R)_2$-MBA_2CuBr_4 chiral perovskite thin film. J. Phys. Chem. Lett. 2025;16(39):7540–7550.
[24] Podgorbunskii KH, Kuleshov T, Ryzhkov D, Lempskii O, Bychkov. Mechanical amorphization of chitosan with different molecular weights. 2022;14(20):4438.
[25] Braglya M, Bistac S, Binder D. Adsorption and structuration of PEG thin films: Influence of the substrate chemistry. 2024;16(9):1244.

[26] Queiroz LPO, Maia E, Aroucha M, dos Santos FKG, et al. Influence of alginate extraction conditions from the brown seaweed Dictyota mertensii on the functional properties of a novel glycerol plasticized alginate film. Carb. Polym. 2025; 352:123225.
[27] Hassani A, Mahdi M, Azarash S, Hussain SA. Preparation, characterization and therapeutic properties of gum Arabic-stabilized gallic acid nanoparticles. Sci. Rep. 2020; 10:17808.
[28] Zhang HP, Cao JD, Jiang WB, Yang YQ, et al. Synthesis and mechanical properties of poly acrylamide gel doped with graphene oxide. Energies. 2022; 15(15):5714.
[29] Strykerus A, Abouhager A, Kissmyte-Snioke M, et al. Development and characterization of a gelatin-based photoactive hydrogel for biomedical application. J. Funct. Biomater. 2025;16(2):43.
[30] Nanda D, Behera D, Pattnaik SS, et al. Advanced in natural polymer-based hydrogels: Synthesis, applications and future directions in biomedical and environment fields. Discov. Polym. 2025;2(6):1–29.
[31] Singh V. Thermophysical study of chitosan-starch-glutamic acid film in acetic acid-water mixture. J. Appl. Mat. Sci. 2026; 2:260104.
[32] Yadav M, Maurya P, Dash P, Seth A, Yadav D, et al. Development of UV-resistant chitosan/starch biofilms reinforced with chitosan nanoparticles for sustainable packaging. Polymers. 2026;18(5):642.
[33] Jia S, Bao D, Han N, Liu Z, et al. Thermal-regulated sodium alginate-g-mPEG fibers with stable shape and high enthalpy value prepared by in-situ wet spinning method. J. Energy Stor. 2024; 87:11411.
[34] Ibrahim SM. Arabic gum grafted PEGDMA hydrogels: synthesis, physicochemical characterization and in-vitro release of hydrophobic drug. Macromol. Res. 2020; 28:1220–1231.
[35] Chen M, Liu J, Lin J, Zhuang K, Shan Y, et al. Progress in polysaccharide-based hydrogels for preventing postoperative adhesions. Gels. 2025;11(3):188.
[36] Ramos P, Bryoncel M. Influence of storage conditions on the stability of gum Arabic and tragacanth. Molecules. 2022;27(5):1510.
[37] Elbedweehy AM, Atta AM. Novel superadsorbent highly porous hydrogel based on Arabic gum and acrylamide. grafts for fast and efficient methylene blue removal. Polymers. 2025; 17(13): 1861.
[38] Alam S, Sukhan H, Uddin S, Umar A, Zahoor M. Exploring the sorption characteristics of gum Arabic grafted polyacrylamide hydrogel in acid yellow-34 contaminated water. Int. J. Chem. Kinet. 2026; 10: 1002/kin. 70105.
[39] Logigan CL, Delaite C, Tiron CE, Peptu C, et al. Chitosan grafted poly(ethylene glycol) methyl ether acrylate particulate hydrogels for drug delivery applications. Gels. 2022; 8(8): 494.
[40] Loghin DF, Bazargideanu MM, Vasiliu S, Racovita S, et al. Hydrogel beads of amidoximated starch and chitosan as efficient sorbents for inorganic and organic compounds. Gels. 2022; 8(9): 549.
[41] Valle-Bravo AV, Camacho-Diaz BH, Rodrigue D, et al. Effect of mechanical homogenization on nopal mucilage for the treatment of a real cyanidation barren solution. Gels. 2026; 12(7): 569.
[42] Mehryou A, et al. Sodium alginate/polyvinyl alcohol semi-interpenetrating hydrogels reinforced with PEG-grafted-graphene oxide. Int. J. Biol. Macromol. 2024; 263(2): 430258.
[43] Singh J, Singh B, Vishavnath. Designing starch-alginate hydrogels for controlled delivery of fungicide for the alleviation of environment pollution. ACS Agric. Sci. Technol. 2022; 2(6): 1239-1250.
[44] Wang Y, Zhou X, He L, Zhou X, Wang Y, Zhou P. Research progress on using modified hydrogel coatings as marine antifouling materials. Mar. Drugs. 2024; 22(12): 546.
[45] Eltaboni F, Ibrahim M. Hydrogels based on gum Arabic and potassium alum. Int. J. New Chem. 2025; 12(3): 264-282.
[46] Jabrail FH, Mahmood ME. Hydrophilic monomers graft gum Arabic hydrogels prepared in different cross-link nature and study of their effect on irrigation of agricultural soil. Res J Chem Sci. 2016; 6(1): 22-37.